Journal Pre-proof

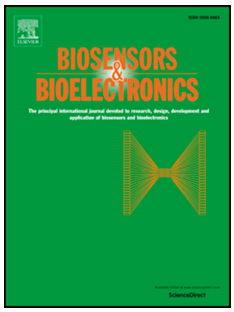

Dual-amplified strategy for ultrasensitive electrochemical biosensor based on click chemistry-mediated enzyme-assisted target recycling and functionalized fullerene nanoparticles in the detection of microRNA-141

Lili Zhou, Ting Wang, Yan Bai, Yi Li, Juhui Qiu, Wen Yu, Sheng Zhang

PII: S0956-5663(19)31041-3

DOI: https://doi.org/10.1016/j.bios.2019.111964

Reference: BIOS 111964

To appear in: *Biosensors and Bioelectronics*

Received Date: 21 October 2019

Revised Date: 10 December 2019

Accepted Date: 12 December 2019

Please cite this article as: Zhou, L., Wang, T., Bai, Y., Li, Y., Qiu, J., Yu, W., Zhang, S., Dual-amplified strategy for ultrasensitive electrochemical biosensor based on click chemistry-mediated enzyme-assisted target recycling and functionalized fullerene nanoparticles in the detection of microRNA-141, *Biosensors and Bioelectronics* (2020), doi: https://doi.org/10.1016/j.bios.2019.111964.

Author Contributions Section

Lili zhou: Generating ideas; Formulation or evolution of overarching research goals and aims; Development or design of methodology; Preparation, creation and presentation of the published work; Writing the initial draft

Ting Wang: Scrub data and maintain research data; Writing- Original draft preparation

Yan Bai: Writing the initial draft; Application of statistical

Yi Li: Writing- Original draft preparation; Participate in the experiment of electrophoresis characterization

Juhui Qiu: Conducting a research and investigation process; Provision of study materials, reagents, materials, patients, laboratory samples

Wen Yu: Preparation, creation and presentation of the published work by those from the original research group

Sheng Zhang: Writing- Original draft preparation, Data curation, Oversight and leadership responsibility for the research activity planning and execution, including mentorship external to the core team

CRediT author statement

Lili zhou: Conceptualization, Methodology, Software

Ting Wang: Data curation, Writing- Original draft preparation

Yan Bai: Formal analysis

Yi Li: Writing- Original draft preparation, Methodology

Juhui Qiu: Resources, Investigation

Wen Yu: Writing- Original draft preparation

Sheng Zhang: Writing- Original draft preparation, Data curation, Supervision

Dual-amplified strategy for ultrasensitive electrochemical biosensor based on click chemistry-mediated enzyme-assisted target recycling and functionalized fullerene nanoparticles in the detection of microRNA-141

Lili Zhou [a, b, *], Ting Wang [a, c], Yan Bai [a, b], Yi Li [a], Juhui Qiu [d], Wen Yu [a], Sheng Zhang [e, *]

[a] Key Laboratory of Laboratory Medical Diagnostics of Education, Department of Laboratory Medicine, Chongqing Medical University, Chongqing 400016, P. R. China

[b] Department of Clinical Laboratory, People's Hospital of Changshou Chongqing, Chongqing 401220, P. R. China.

[c] Department of Clinical Laboratory, The Central Hospital of Fuling Chongqing, Chongqing 408099, P. R. China

[d] State Key Laboratory of Membrane Biology, Tsinghua-Peking Center for Life Sciences, School of Life Sciences, Tsinghua University, Beijing 100084, P. R. China.

[e] School of Economics and Management, Chongqing University of Posts and Telecommunications, Chongqing 400065, P. R. China

*Corresponding author.

E-mail addresses: lilizhou_cqmu@163.com;

Abstracts: Rapid and efficient detection of tumor marker at the early stages is one of the crucial challenges in cancer diagnostics and therapy. In this study, an ultrasensitive electrochemical biosensor was fabricated by dual-amplified strategy for the detection of ultra-trace microRNA-141 (miRNA-141). Firstly, two split sequences contained G-quadruplex were connected by click chemistry-mediated nucleic acid strands self-assembly and the obtained complete G-quadruplex was complementary with miRNA-141 to formed DNA-RNA hybrid duplexes. Subsequently, the formed DNA-RNA hybrid duplexes were specifically recognized by duplex-specific nuclease (DSN), and the DNA part of the duplexes were cleaved and the miRNA-141 were released to trigger next cycle, which acquired a primal signal amplification by enzyme-assisted target recycling (EATR). Moreover, amino and thiol group multi-labeled functionalized fullerene nanoparticles (FC60) with a larger surface active sites and better biocompatibility, were designed rationally to modify the Au electrodes, which produced multiply-enhanced amplified signal. This dual-amplified sensing system exhibited a remarkable analytical performance for the detection of miRNA-141 in concentrations ranging from 0.1 pM to 100 nM and the detection limit of 7.78 fM was obtained. Compared with the biosensor with single amplification strategy such as EATR, this

electrochemical biosensor based on dual-amplified strategy exhibited an excellent discrimination capability and higher analytical performance. Therefore, this electrochemical biosensor might hold a great potential for further applications in biomedical research and early clinical diagnosis.

Keywards: Enzyme-assisted target recycling; DNA nanotechnology; Copper (I)-catalyzed azide-alkyne cycloaddition; Duplex-specific nuclease; Functionalized fullerene nanoparticles; MicroRNA-141

1. Introduction

Cancer is one of main factors to cause death all over the world (Mirzaei et al. 2016a; Mirzaei et al. 2016b). The early-diagnosis for cancer plays an essential role in reducing the morbidity and mortality, and avoiding long-term ineffective treatments and side-effects (Jackson and Bartek 2009; Wilson and Hay 2011). Therefore, finding highly selective biomarkers which can provide much accurate information and efficiency for monitoring the occurrence and development of cancer is urgent (Hashemi Goradel et al. 2018). Notably, microRNAs (miRNAs) are a class of small-sequence and endogenous noncoding RNA (typically 19-22 nucleotides), which can regulate the expression of specific genes at post-transcriptional level (Shabaninejad et al. 2019; Tavakolizadeh et al. 2018; Yates et al. 2013). Thus, the expression of miRNAs and their quantitative expression profiles may be used as the potential biomarkers

to predict disease occurrence and progression (George et al. 2013; Whatley et al. 2013). For this regard, a variety of methods for the detection of miRNAs were developed, i.e. northern blotting (Válóczi et al. 2004), real-time polymerase chain reaction (RT-PCR) (Verdoy et al. 2012), microarrays (Li and Ruan 2009) and miRNAs next-generation sequencing (Volinia et al. 2012).It remains an arduous challenge to improve the technical for the ultrasensitive detection and specific analysis of circulating miRNAs due to their small size, low-abundance as well as the sequence similarity among their family members (Tavallaie et al. 2018).

Compared with the traditional analysis strategies, the development of biosensors attracted more attention in the high selectivity, high sensitivity, low-cost and easy operation (AbduláRasheed 2015; Yang et al. 2016). The DNA nanotechnology combined the advantages of nanotechnology and nucleic acids to provide a new strategy of signal amplification for the biosensors in early diagnosis (Yan 2004). In this technology, DNA can not only use as rigid chain to construct highly-ordered structure at the nanoscale programmable, but also utilize the controllable and predesigned manner to bind with various nanomaterials, such as carbon nanomaterials, Au nanoparticles (AuNPs) and quantum dots (QDs), to produce stable and amplified signal (Seeman 2003; Wang et al. 2018). In DNA nanotechnology, the autonomous

synthesis of the double helix is based on strict rules of base pairing that allow portions of the strand to be predictably connected based on their sequence. This 'selective stickiness' is a key advantage in the construction of DNA machinery. However, this biologic conjugation process needs strict reaction condition to boycott the non-specificity combination. For instance, the ion-bridged complexes formed between base pairs, T-Hg^{2+}-T or C-Ag^{+}-C bridges (Miyake et al. 2006). To address this insufficiency, various attempts have been made to chemically synthesize new oligonucleotide conjugates with diverse functionalities. Among this reaction, the copper (I)-catalyzed azide-alkyne cycloaddition (CuAAC) reaction is an outstanding representative of the click reactions, which are characterized by high yield, mild reaction condition, and extremely high compatibility with functional groups (Rostovtsev et al. 2002). The CuAAC reaction has previously been widely utilized for nucleic acid labeling, conjugation and detection (Gramlich et al. 2008). To achieve ultra-trace miRNAs detection, many amplification strategies have been developed via the amplification of targets, probes or signals, such as catalytic hairpin assembly amplification (Li et al. 2015), target-recycled enzyme-free amplification (Loo et al. 2016), exponential amplification reaction (Fan et al. 2018) and enzymatic amplification (Xu et al. 2012). Other effective amplification method is the nanomaterials-based sensors, such as carbon nanomaterials, because of its notable electronic properties

and the possibility to perform precise chemical modification, which prompt have potential applications valuable in various physical, chemical and biomedical fields (Chen and Dai 2013).

Inspired by above findings, we developed dual-amplified strategy for the detection of low quantity miRNA-141 by integrating click chemistry-mediated enzyme-assisted target recycling (EATR) with amino and thiol groups multi-functionalized fullerene nanoparticles(FC60). Two breaches nucleic acid chains contained G-quadruplex DNA sequences were connected by click chemistry and the obtained DNA hairpin loop was complementary with the target sequence to hybrid formed DNA-RNA duplexes. Herein, the forming DNA-RNA duplexes were cleaved by duplex-specific nuclease (DSN). As DSN showed a satisfactory ability to discriminate between well-matched and mis-matched duplex DNA (least single-base mis-match), so the DNA in the DNA-RNA duplexes were cleaved and the free miRNA were released to trigger another cycle and achieve the exponential amplification of the signal (Hao et al. 2015; Zhao et al. 2007). Moreover, we rationally designed FC60, which were used to modify the Au electrodes and further amplified the detection signal. The experimental results indicated that, compared with the biosensor with single amplification strategy, this electrochemical biosensor based on EATR and FC60 exhibited an excellent discrimination capability and higher analytical performance,

which might hold a great potential for further applications in biomedical research and early clinical diagnosis.

2. Experimental

2.1. Chemicals and materials

All HPLC-purified DNA oligonucleotides sequences were synthesized by Sangon Biotechnology Inc. (Shanghai, China). MiRNA-141, miRNA-21, miRNA-200a, miRNA-200b and let-7a were obtained from TaKaRa Biotechnology Co., Ltd. (Dalian, China). The nucleic acid sequences were listed in Table S1. $CuCl_2$•$2H_2O$, [Copper (II) chloride dihydrate], sodium ascorbate, hemin, and 30 % H_2O_2 (hydrogen peroxide) were purchased from Sigma-Aldrich (St. Louis, MO, USA). Tris (hydroxymethyl) aminomethane-hydrochloride (Tris-HCl), 6-mercapto-1-hexanol (MCH, 97 % purity), toluene ($C_6H_5CH_3$), 3, 4, 9, 10-perylenete-tracarboxylic dianhydride ($C_{24}H_8O_6$, PTCDA), anhydrous ethylenediamine, N-(3-dimethylaminopropyl)-N′-ethylcarbodiimide hydrochloride (EDC), N-hydroxy succinimide ester (NHS) and L-cysteine (Cys) were supplied from Aladdin Chemistry Co., Ltd. (Shanghai, China). Fullerene (C60) with purity > 99.9 wt % was obtained in Nanjing Xianfeng Nano Co. (Nanjing, China). Duplex-specific nuclease (DSN) was purchased from Evrogen Joint Stock Company (Russia). All reagents were of analytical grade and used without further

purification. All solutions were prepared using ultrapure water (≥ 18.2 MΩ cm, Milli-Q, Millipore System Inc).

2.2. Apparatus

All electrochemical measurements, including differential pulse voltammograms (DPV), cyclic voltammetry (CV) and electrochemical impedance spectroscopy (EIS) were performed with a CHI 660E electrochemical workstation (Shanghai Chenhua Instrument, China). A conventional three-compartment electrochemical cell was employed for all electrochemical measurements, which including a modified Au electrode (3 mm in diameter) as working electrode, a KCl-saturated Ag/AgCl electrode as reference electrode and a platinum wire as auxiliary electrode. A NanoDrop 1000 UV-visible spectrophotometer (Thermo, USA) was used to analysis the properties of C60 and FC60. The morphologies of nanocomposites were obtained by Transmission electron microscopy (TEM) (ZEISS LIBRA 200, Carl Ziess, GmbH, Germany). X-ray photoelectron spectroscopy (XPS) was introduced to analyze the nanoparticle surface composition using Thermo Scientific Escalab 250Xi (Rockford, IL, America)

2.3. Preparation of C60 aqueous solution and FC60

The C60 aqueous suspension was prepared by solvent-exchange

method according to previous literature with minor modifications (Brant et al. 2005; Hilburn et al. 2012) (Fig. S4). Firstly, C60 powder (3 mg) was added into 3 mL of toluene, with the reaction progresses gradually generated purple C60 toluene solution. Then, 3 mL of ultrapure water was mixed into the purple solution and the mixture would become stratified. Next, the two-phase liquid-liquid mixture was treated by ultrasonic waves for several hours, until made toluene adequately volatilized and C60 transferred to aqueous phase from toluene phase. And the brown C60 aqueous solution was obtained. The synthesis of FC60 was performed in the following approach according to reported (Han et al. 2013). Firstly, 10 mg of PTCDA was dissolved in 2 mL of ethanol with stirring, and then 20 mL of anhydrous ethylenediamine was gradually poured into above solution under 4 °C. After stirring for 2 h, the procreant PTC-NH_2 was centrifuged and washed extensively with acetone and ethanol, and finally kept in a vacuum at room temperature for drying. Then, 1 mg of PTC-NH_2 was added into 1 mL of the prepared C60 suspension with ultrasonic dispersion for 2-3 h to obtain the amido group functionalized C60 (PTC-NH_2-C60). The obtained product was washed adequately with ultrapure water and collected by centrifugation. Finally, the Cys solution was activated by EDC and NHS to increase active groups of PTC-NH_2-C60, and then PTC-NH_2-C60 was added, the mixture was reacted overnight under violently stirring to generate the amino and thiol

groups functionalized C60. The resultant product was centrifugation at 12,000 rpm for 15 min to remove surplus Cys solution, then resuspended the FC60 sediment in ultrapure water and stored at 4 °C for further use.

2.4. Preparation of click chemistry-mediated EATR

Azide-modified DNA strand (azide-strand) and alkyne-modified DNA strand (alkyne-strand) were dissolved in 1×TE buffer (10 mM Tris-HCl, 1 mM EDTA, pH 7.5). 80 μL of azide-strand and 20 μL of alkyne-strand (4:1 v/v) were mixture in micro-centrifuge tube (0.5 mL), the final concentration of DNA strand was 1 μM (Fig. S1 and Fig. S2). Then added 1.2 μL of 10 mM $CuCl_2$•$2H_2O$ solution and 0.8 μL of 10 mM sodium ascorbate solution, shocked for 2 h at room temperature (RT, 25 ± 2 °C). After the reaction, we got the complete G-quadruplex DNA sequences by CuAAC catalyzing. Different concentrations of miRNA-141 were mixed with CuAAC reaction mixture and heated at 95 °C water bath for 5 min. Following by slowly cool to room temperature two hours before the experiment to adequately hybridized between the alkyne-strand and target, and to form duplex structure (DNA-RNA duplex). Finally, 0.5 U DSN was added into above solution and incubated in 60 °C for 30 min.

2.5. Electrochemical biosensor construction

The method of pretreatment Au electrode was followed the previous works of our team (Wang et al. 2016). After the cleaning procedure, 10 μL homogeneous suspension of FC60 was dropped on the pretreated Au electrode surface making it fully dispersed and allowed to dry in air. The FC60 was immobilized on the Au electrode surface via the Au-S bonds between the Au surface and the thiol groups of FC60. Then, the modified Au electrodes were thoroughly cleaned with phosphate buffer (pH 7.0, 0.01 M) and ultrapure water respectively. Next, the EATR reaction product (10 μL) was dropped on the modified Au electrodes surface, and then incubated for overnight at 4 °C. Finally, immobilized the generated horseradish peroxidase (HRP)-mimicking DNAzyme (G-quadruplex sequence) through condensation reaction between the carboxyl groups of nucleic acids and the amino groups of FC60.

3. Results and discussion

3.1. Principle of proposed biosensor for miRNA-141 detection

The working principle of this dual-amplified strategy biosensor platform for ultrasensitive detection of miRNAs was depicted in Scheme 1. To verify the feasibility of this dual-amplified strategy, the miRNA-141 was selected as the model target to test whether or not our design functions as intended. The miRNA-141 can be used as a potentially diagnostic biomarker of prostate cancer (PC), which has been found to be

up-regulated in PC specimens (Gonzales et al. 2011). Alkyne-strand was first incubated in 95 °C bath for 5min to form hairpin structure for blocking the split G-quadruplex sequence included in it and reducing the background signal. Azide-strand and hairpin alkyne-strand were linked by CuAAC reaction to constitute the cDNA capture probe contained a complete G-quadruplex sequence. Herein, the DNA-RNA hybrid duplexes were formed by a self-assemble process with cDNA to capture target miRNA. When incubated with hybrid duplexes and DSN, the EATR reaction was triggered with the special binding of DNA and miRNAs, and the DNA part in the DNA-RNA well-matched hybrid duplexes were cleaved selectively by DSN and the free miRNA-141 was released to trigger another cycle due to the DSN inactive towards ssRNA (Li et al. 2016). After the EATR reaction, produced the extremely abundant complete G-quadruplex, this sequence will form horseradish peroxidase (HRP)-mimicking DNAzyme in the presence of hemin and K^+. The FC60 immobilized on the surface of Au electrodes was hybridized with the G-quadruplex sequence to produce an enhanced electrochemical signal. Remarkable, there was no target miRNAs, the alkyne-strand was remained the hairpin structure and closed a part of G-quadruplex sequence, the FC60 hybridized with CuAAC reaction production would not show an electrochemical signal.

<Scheme 1>

3.2. PAGE characterization of the EATR

Native polyacrylamide gel electrophoresis (PAGE) was first used to verify this dual-amplified detection strategy. As shown in Fig. 1, the mixture of azide-strand and alkyne-strand exhibited a clear band (lane 3) at the position of above only azide-strand (lane 1) and alkyne-strand (lane 2), indicating the successfully conjugated between azide-strand and alkyne-strand mediated by CuAAC reaction. Remarkably, in lane 1 was not observed obvious nucleic acid bands, the reason may be due to the length of azide-strand was too short (9 nt) and run over the electrophoretic gel when electrophoresis. The incubation of target strand with the mixture of CuAAC produce resulted in the appearance of a band (lane 4) above the lane 3, indicating the hybridization between the target and the loop part of alkyne-strand. When DSN was added into the mixture solution containing the azide-strand, alkyne-strand and target strand, a band with reduced mobility was observed (lane 5) due to the cleaving action of DSN to DNA in the DNA-RNA duplex.

<Fig. 1>

3.3. Characterization of the C60 and FC60

The characterization of the carbon nanomaterials including morphologies, size and the preparation were shown in Supporting

Information. The zeta potential increased from a relatively large negative value (−29 ± 0.5 mV) to −25.4 ± 0.5 mV upon amino and thiol groups functionalized (Fig. S6). Additionally, the typical TEM image demonstrated that C60 exhibited a well-defined shape of spheres structures with a diameter of 80 ± 20 nm (Fig. S7A), indicating the successfully preparation of C60 nanoparticles. The morphology of FC60 (Fig. S7B) is somewhat irregularly shaped with the homogeneous distribution and the size of FC60 is become about two times for C60. This results demonstrated above indicate that the FC60 has been synthesized as expected.

XPS characterization was also employed for elemental analysis in order to further investigate the successful synthesis of FC60. As shown in Fig. 2, the XPS survey spectrum for C60 and FC60. As expected, FC60 contains C, N, S and O elements. The regional C1s spectrum can be differentiated into three peaks with binding energies at 284.1, 285.3 and 288.8 eV, respectively (Fig. 2 c and d). The main C1s peak located at 284.1 eV is assigned to adventitious carbon and sp2 carbon from the C60. The peak located at 285.3 eV is attributed to defect containing sp2 carbon (Liu and Zeng 2008; Wang and Zhang 2012). In addition, there is a relatively weak peak located at 288.8 eV, corresponding to carboxyl carbon (O=C–O) (Chen et al. 2012). The peak at about 400 eV (shown in Fig. 2b) is ascribable to C-NH_2 (Cong et al. 2013). The O1s XPS

spectrum illustrated in Fig. 2e can be differentiated as following peaks, the peak at 531.8 eV is ascribable to C=O and O–C=O species, and the peaks at 532.5 eV are ascribable to O1s (Mattevi et al. 2009). The peak located at 163.3 eV (Fig. 2f) is attributed to defect containing S2p sulfur (Zhao et al. 2015). The results of XPS further validate the successful synthesis of FC60.

<Fig. 2>

3.4. Electrochemical characterization of this biosensor

The stepwise fabrication of this sensing platform was verified by cyclic voltammetry (CV) and electrochemical impedance spectroscopy (EIS). CV measurements were employed to characterize the changes in electrochemical properties during the modification process. As exhibited in Fig. 3A, a well-defined redox pair was observed, showing a fast electron-transfer kinetics of $[Fe\text{-}(CN)_6]^{3-/4-}$ on the bare Au electrode (curve a). After the immobilization of FC60 on the Au electrode surface, a significantly reduced current signal was obtained (curve b), resulted by the electrostatic repulsion between the negatively charged FC60 and $[Fe\text{-}(CN)_6]^{3-/4-}$. The current response further decreased and the separation degree of two peaks was enlarged after the self-assembling process of DNA molecules (curve c), caused by the electrostatic repulsion between the negatively charged deoxyribose-phosphate backbone of DNA

molecules and $[Fe\text{-}(CN)_6]^{3-/4-}$, indicating the successful immobilization of DNA molecules. To eliminate the non-adsorbed DNA molecules and hold a good orientation of DNA, MCH was assembled onto the DNA modified Au electrode, and large decrease in peak currents and enlarged peak-to-peak separation could be observed (curve d). This could be related to the blocking effect of MCH to the permeation of redox species to the surface of the electrode. All the CV data above indicated the successful fabrication of the electrochemical biosensor.

Electrochemical impedance spectroscopy (EIS) technology was also used to monitor properties of the stepwise modified Au electrode. The curves of EIS presented as the Nyquist plot consisted of two portions: the diameter of semicircle at higher frequencies represented the electron-transfer resistance (Ret), the linear part at lower frequencies corresponding to the diffusion-limited process held in solution. The EIS data were fitted according to a Randles equivalent electrical circuit based on ZSimpWin software ($ChiSq=8.1\times10^{-4}$) (inset, Fig. 3B). The equivalent electrical circuit consisted of an active electrolyte resistance (Rs) in a series with a constant phase element (CPE) and an electro-transfer resistance (Ret) in parallel with Warburg impedance (ZW). As shown in Fig. 3B, a significant difference in the Ret obtained from each surface modification step. Bare Au electrode exhibited a small semicircle portion (curve a) due to the feasible access of the electro-active species

354 $[Fe\text{-}(CN)_6]^{3-/4-}$ to the electrode surface. Increase in the Ret for the FC60
355 immobilized electrode (curve b) revealed that FC60 hindered the electron
356 transport from the solution to the electrode surface, suggesting the
357 successful assemblage of FC60. Further increment in Ret value can be
358 obtained after nucleic acid has been immobilized on the FC60, was
359 attributed to the deoxyribose-phosphate backbone with abundant negative
360 charges, resulting in the electrostatic repulsion between $[Fe\text{-}(CN)_6]^{3-/4-}$
361 and electrolytic solution which inhibit electron transport flow (curve c).
362 After the immobilization of MCH, a large increase in Ret was observed
363 (curve d), due to the blocking of MCH with non-conductive properties
364 prevented the electron transfer. The variation in EIS were in agreement
365 with those in the CV method, which further demonstrated the success of
366 each modification step.

367 <Fig. 3>

368

369 **3.5. Electrochemical responses of the biosensor toward miRNA-141**

370 To evaluate the dependence of current intensity upon the
371 concentration of miRNA-141, the developed biosensor was incubated
372 with different concentrations of miRNA-141 and then detected in the
373 working buffer (PBS, pH 7.0 containing 1.05 mM H_2O_2). As shown in
374 Fig. 4, the current signal increased with the increase of target
375 concentrations. According to the calibration plots of current intensity to

logarithm C_T in Fig. 4A and 4B, when the biosensor was not modified the FC60, a linear regression equation was ΔI (μA) = $-1.091 \log_{10} C_T - 4.296$ with a coefficient of determination (R^2) of 0.9903, where ΔI stands for the current variation and C_T stands for the concentration of target miRNA-141 (n = 3). The detection limit was estimated at 0.122 pM (S/N = 3). In order to elucidate the FC60 effect on amplification efficiency, the DPV assays were performed using the carboxyl-modified azide-strand instead of thiol-modified azide-strand under the FC60 modified Au electrode. As a result, the linear ranges from 0.1 pM to 100 nM was achieved for miRNA-141 with detection limit of 7.78 fM (Fig. 4C and 4D) corresponding to three times the average standard deviation of the blank response, which provided an effective evidence for the sensitivity improvement of proposed dual-amplified strategy. Thus, this biosensor could be applied to quantification of nucleic acids with a wide linear range and low detection concentration.

<Fig. 4>

The specificity of the proposed electrochemical sensor was evaluated by detecting five different kinds of control miRNAs sequences, including complementary target (miRNA-141), miRNA-200a, miRNA-200b, miRNA-21 and let-7a at the same condition. As shown in Fig. 5A, the DPV currents for 1 nM of miRNA-200a, 1 nM of miRNA-200b, 1 nM of miRNA-21 and 1 nM of let-7a were all similar to

that of the blank. However, in the presence of miRNA-141 at the concentration of only 0.1 nM, there was a remarkable increase in the DPV current, which was about 4 times as that of miRNA-200a and miRNA-200b and 9 times as that of miRNA-21 and let-7a (Fig. 5A). In addition, the reproducibility of prepared biosensor was further investigated by measuring the target miRNA from 0.01 nM to 100 nM with three replicates, respectively (Fig. 5B). It can calculate that the relative standard deviation (RSD) was about 2.9%. Therefore, the designed electrochemical sensor was able to effectively detect the target nucleic acids with high specificity and good reproducibility by the dual-amplified strategy and had great potential for clinical analysis.

<Fig. 5>

4. Conclusions

In summary, a novel sensing system was successfully designed to construct a label-free and highly sensitive electrochemical biosensor for nucleic acids detection based on click chemistry-mediated EATR and FC60 dual-amplified strategy. In order to reduce false positive results, the unnecessary ion bridge connection of the nucleic acid was avoided effectively by using the CuAAC reaction. The improvement of analytical properties was ascribed to specificity of hairpin alkyne-strand, CuAAC and DSN, and good amplification of both EATR and FC60. Moreover, the

proposed electrochemical biosensor can also be conveniently applied for other nucleic acids analysis simply by altering the corresponding DNA sequences of alkyne-strand. The CuAAC reaction used in this strategy has the potential to analyze Cu^{2+} in body fluid. Therefore, the easy operation, high sensitivity, high selectivity and better universal of this proposed biosensor platform has a great potential for further applications in early clinical diagnosis, biomedical research, food safety, and environmental monitoring.

Acknowledgements This work was financially supported by the Natural Science Research Foundation of China (81171415, 81802110 and 81902169) and Chongqing Changshou District Science and Technology Project (CS2019031)

References

AbdulaRasheed, P., 2015. Analyst 140(8), 2713-2718.
Brant, J., Lecoanet, H., Wiesner, M.R., 2005. J. Nanopart. Res. 7(4-5), 545-553.
Chen, L., Chen, F., Shi, Y., Zhang, J., 2012. J. Phys. Chem. C 116(15), 8579-8586.
Chen, T., Dai, L., 2013. Mater. Today 16(7-8), 272-280.
Cong, C.-b., Cui, C.-c., Meng, X.-y., Lu, S.-j., Zhou, Q., 2013. Chem. Res. Chinese U 29(4), 806-810.
Fan, T., Mao, Y., Sun, Q., Liu, F., Lin, J.S., Liu, Y., Cui, J., Jiang, Y., 2018. Cancer Sci. 109(9), 2897.
George, S., Chaudhery, V., Lu, M., Takagi, M., Amro, N., Pokhriyal, A., Tan, Y., Ferreira, P., Cunningham, B.T., 2013. Lab. Chip. 13(20), 4053-4064.
Gonzales, J.C., Fink, L.M., Goodman Jr, O.B., Symanowski, J.T., Vogelzang, N.J., Ward, D.C., 2011. Clin. Genitourin. Canc. 9(1), 39-45.

Gramlich, P.M., Wirges, C.T., Manetto, A., Carell, T., 2008. Angew. Chem. Int. Edit. 47(44), 8350-8358.

Han, J., Zhuo, Y., Chai, Y., Yuan, R., Xiang, Y., Zhu, Q., Liao, N., 2013. Biosens. Bioelectron. 46, 74-79.

Hao, N., Dai, P.-P., Yu, T., Xu, J.-J., Chen, H.-Y., 2015. Chem. Commun. 51(70), 13504-13507.

Hashemi Goradel, N., Ghiyami□Hour, F., Jahangiri, S., Negahdari, B., Sahebkar, A., Masoudifar, A., Mirzaei, H., 2018. J. Cell. Physiol. 233(4), 2902-2910.

Hilburn, M.E., Murdianti, B.S., Maples, R.D., Williams, J.S., Damron, J.T., Kuriyavar, S.I., Ausman, K.D., 2012. Colloid. Surface. A 401, 48-53.

Jackson, S.P., Bartek, J., 2009. Nature 461(7267), 1071.

Li, W., Jiang, W., Ding, Y., Wang, L., 2015. Biosens. Bioelectron. 71, 401-406.

Li, W., Ruan, K., 2009. Anal. Bioanal. Chem. 394(4), 1117-1124.

Li, Y., Zhang, J., Zhao, J., Zhao, L., Cheng, Y., Li, Z., 2016. Analyst 141(3), 1071-1076.

Liu, B., Zeng, H.C., 2008. Chem. Mater. 20(8), 2711-2718.

Loo, A.H., Sofer, Z., Bouša, D., Ulbrich, P., Bonanni, A., Pumera, M., 2016. ACS Appl. Mater. Inter. 8(3), 1951-1957.

Mattevi, C., Eda, G., Agnoli, S., Miller, S., Mkhoyan, K.A., Celik, O., Mastrogiovanni, D., Granozzi, G., Garfunkel, E., Chhowalla, M., 2009. Adv. Funct. Mater. 19(16), 2577-2583.

Mirzaei, H.R., Mirzaei, H., Lee, S.Y., Hadjati, J., Till, B.G., 2016a. Cancer Lett. 380(2), 413-423.

Mirzaei, H.R., Sahebkar, A., Salehi, R., Nahand, J.S., Karimi, E., Jaafari, M.R., Mirzaei, H., 2016b. J. Cancer Res. Ther. 12(2), 520.

Miyake, Y., Togashi, H., Tashiro, M., Yamaguchi, H., Oda, S., Kudo, M., Tanaka, Y., Kondo, Y., Sawa, R., Fujimoto, T., 2006. J. Am. Chem. Soc. 128(7), 2172-2173.

Seeman, N.C., 2003. Nature 421(6921), 427.

Shabaninejad, Z., Yousefi, F., Movahedpour, A., Ghasemi, Y., Dokanehiifard, S., Rezaei, S., Aryan, R., Savardashtaki, A., Mirzaei, H., 2019. Anal. Biochem. 113349.

Tavakolizadeh, J., Roshanaei, K., Salmaninejad, A., Yari, R., Nahand, J.S., Sarkarizi, H.K., Mousavi, S.M., Salarinia, R., Rahmati, M., Mousavi, S.F., 2018. J. Cell. Biochem. 119(5), 3783-3797.

Tavallaie, R., McCarroll, J., Le Grand, M., Ariotti, N., Schuhmann, W., Bakker, E., Tilley, R.D., Hibbert, D.B., Kavallaris, M., Gooding, J.J., 2018. Nat. Nanotechnol. 13(11), 1066.

Válóczi, A., Hornyik, C., Varga, N., Burgyán, J., Kauppinen, S., Havelda, Z., 2004. Nucleic Acids Res. 32(22), e175-e175.

Verdoy, D., Barrenetxea, Z., Berganzo, J., Agirregabiria, M., Ruano-López, J.M., Marimón, J.M., Olabarría, G., 2012. Biosens. Bioelectron. 32(1), 259-265.
Volinia, S., Galasso, M., Sana, M.E., Wise, T.F., Palatini, J., Huebner, K., Croce, C.M., 2012. P. Nati. A. Sci. 109(8), 3024-3029.
Wang, F., Zhang, K., 2012. Curr. Appl. Phys. 12(1), 346-352.
Wang, T., Zhou, L., Bai, S., Zhang, Z., Li, J., Jing, X., Xie, G., 2016. Biosens. Bioelectron. 78, 464-470.
Wang, Y., Bai, J., Qu, X., Gao, Y., Wang, J., Li, S., Fan, L., Wei, H., Liu, S., Peng, Y., 2018. Nanoscale 10(38), 18354-18361.
Whatley, S.D., Mason, N.G., Rhodes, J.M., Stewart, M.F., Reed, P., Crowley, V., Darby, C.M., Badminton, M.N., 2013. Clin. Chem. 59(7), 1123-1125.
Wilson, W.R., Hay, M.P., 2011. Nat. Rev. Cancer 11(6), 393.
Xu, H., Wang, L., Ye, H., Yu, L., Zhu, X., Lin, Z., Wu, G., Li, X., Liu, X., Chen, G., 2012. Chem. Commun. 48(51), 6390-6392.
Yan, H., 2004. Science 306(5704), 2048-2049.
Yang, H., Gao, Y., Wang, S., Qin, Y., Xu, L., Jin, D., Yang, F., Zhang, G.-J., 2016. Biosens. Bioelectron. 80, 450-455.
Yates, L.A., Norbury, C.J., Gilbert, R.J., 2013. Cell 153(3), 516-519.
Zhao, M., Zhuo, Y., Chai, Y.-Q., Yuan, R., 2015. Biomaterials 52, 476-483.
Zhao, Y., Hoshiyama, H., Shay, J.W., Wright, W.E., 2007. Nucleic Acids Res. 36(3), e14.

Caption

Scheme 1 The schematic diagram of the EATR and FC60 dual-amplified strategy electrochemical biosensor.

Fig. 1 PAGE analysis of different solution. Lane M: 20 bp DNA marker; lane 1: azide-strand (2 μM); lane 2: alkyne-strand (2 μM); lane 3: azide-strand (2 μM) and alkyne-strand (2 μM); lane 4: azide-strand (2 μM), alkyne-strand (2 μM) and miRNA-141 (10 nM); lane 5: azide-strand (2 μM), alkyne-strand (2 μM), miRNA-141 (10 nM) and DSN (0.2 U).

The mixtures were incubated at room temperature.

Fig. 2 XPS analysis for (a) C60; (b) the full region of XPS for FC60; (c) C60-C; (d) FC60-C; (e) FC60-O; (f) FC60-S.

Fig. 3 Characterization of the stepwise modified of the Au electrode. (A) CVs of: (a) bare Au electrode; (b) immobilization of FC60 on the Au electrode; (c) DNA molecules self-assembling on FC60 modified Au electrode; (d) MCH assembled onto the DNA modified Au electrode. (B) EIS of (a) bare Au electrode; (b) immobilization of FC60; (c) DNA molecules self-assembling on FC60 modified Au electrode; (d) MCH assembled onto the DNA modified Au electrode.

Fig. 4 The standards DPV responses (A) and the corresponding calibration curve (B) to 0.001 nM, 0.01 nM, 0.1 nM, 1 nM, 10 nM and 100 nM of target miRNA without FC60 modified the biosensor; DPV responses (C) and the corresponding calibration curve (D) to 0.0001 nM, 0.001 nM, 0.01 nM, 0.1 nM, 1 nM, 10 nM, 20 nM, 30 nM, 50 nM and 100 nM of target miRNA using FC60 modified the biosensor.

Fig. 5 (A) The specificity of the proposed electrochemical biosensor detection of various miRNAs (miRNA-141, miRNA-200a, miRNA-200b,

miRNA-21 and Let-7a); (Each sample was repeated detected three time)

(B) The DPV signal stability of the biosensor to various concentrations of miRNA-141

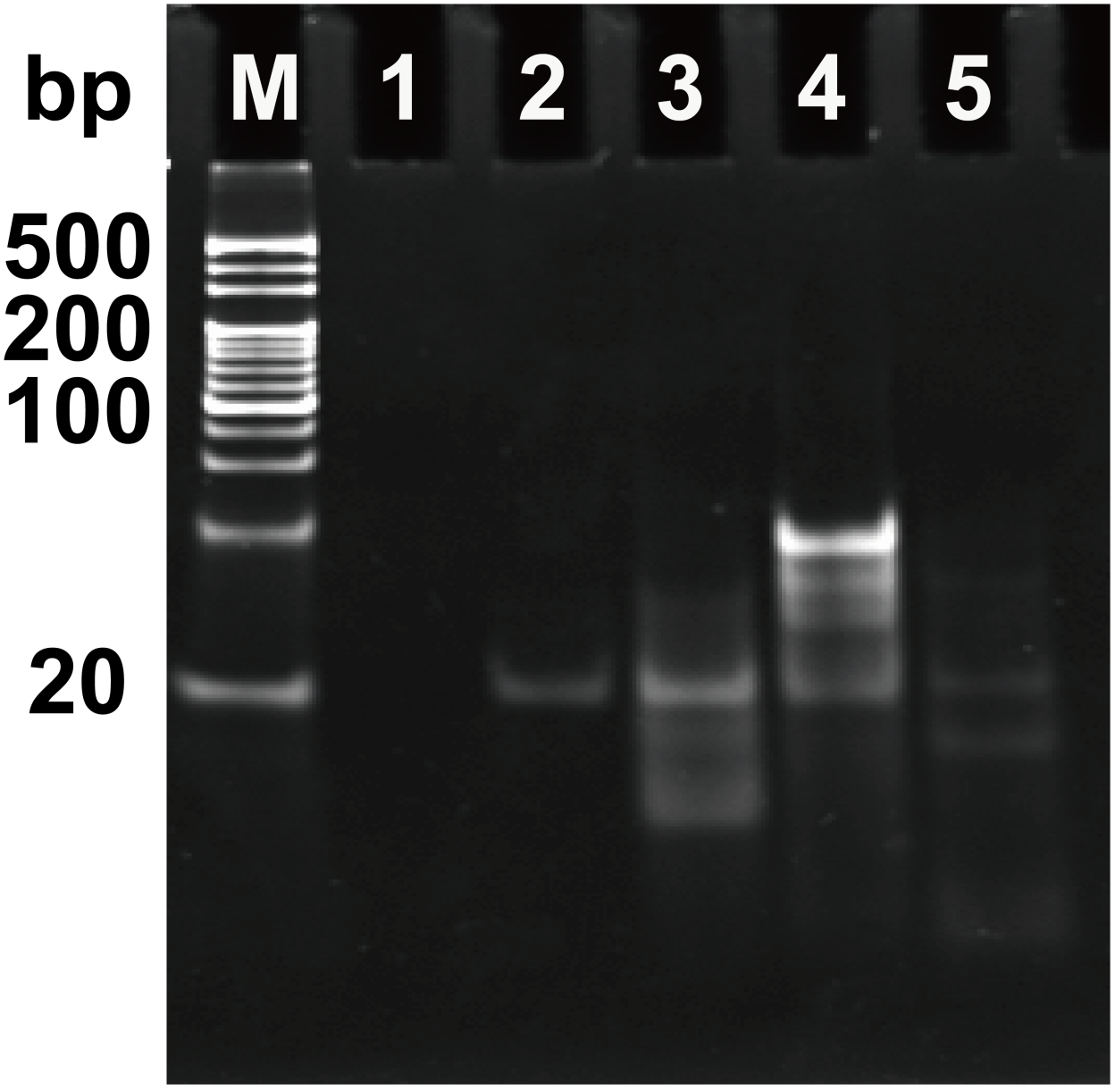
bp
M
1
2
3
4
5
500
200
100
20

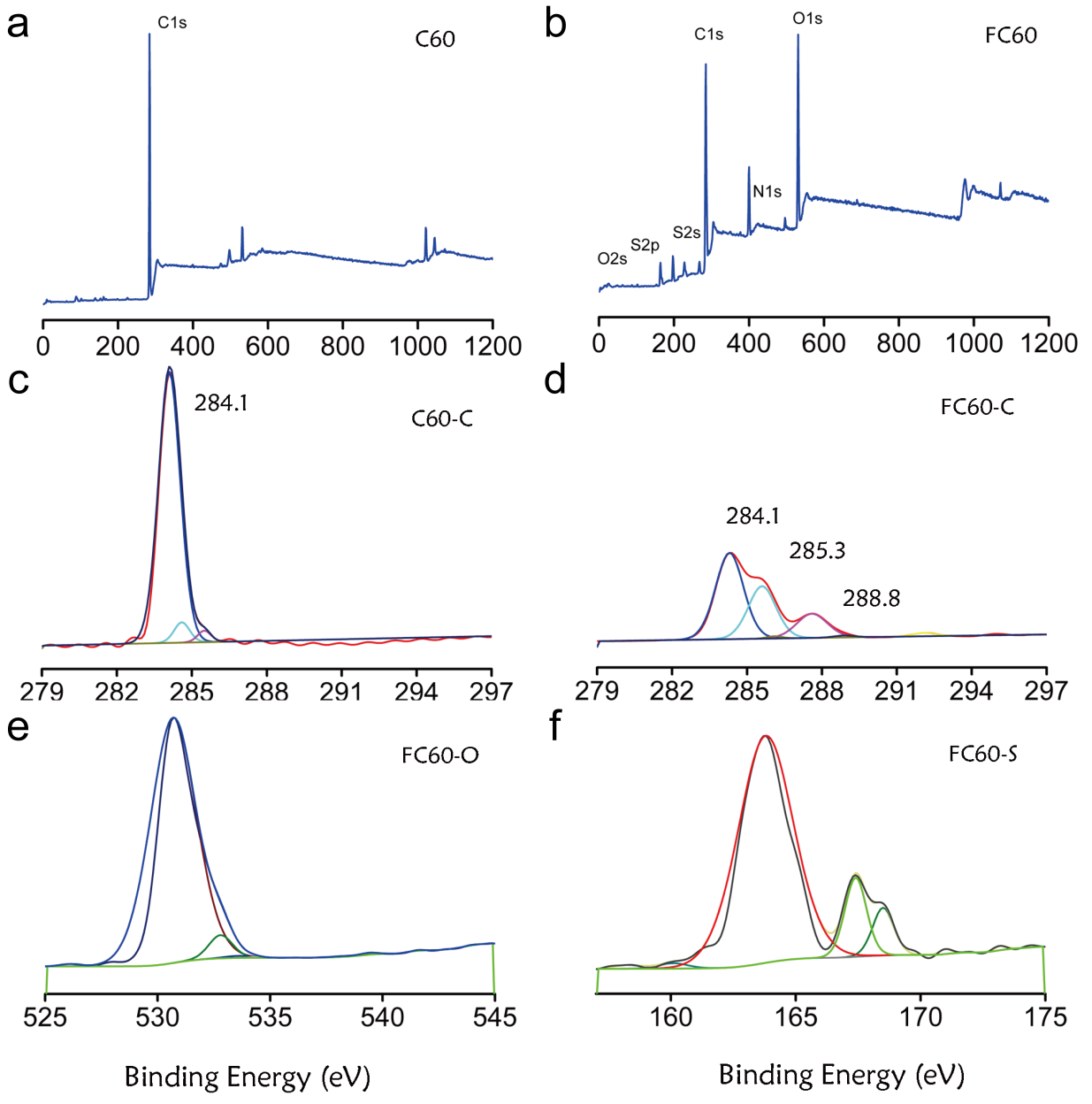
a
C1s
C60
0 200 400 600 800 1000 1200
b
C1s
O1s
FC60
N1s
S2s
S2p
O2s
0 200 400 600 800 1000 1200
c
284.1
C60-C
279 282 285 288 291 294 297
d
FC60-C
284.1
285.3
288.8
279 282 285 288 291 294 297
e
FC60-O
525 530 535 540 545
Binding Energy (eV)
f
FC60-S
160 165 170 175
Binding Energy (eV)

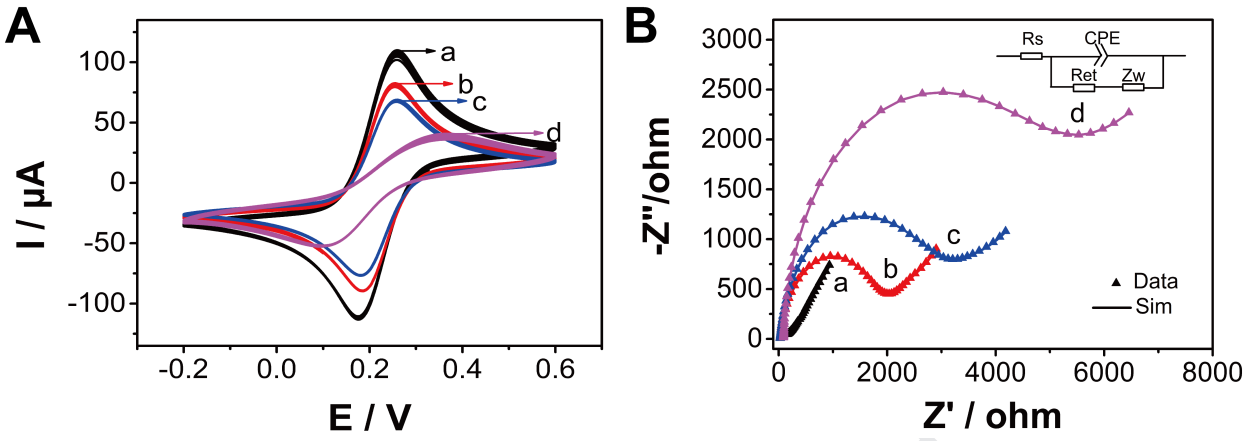

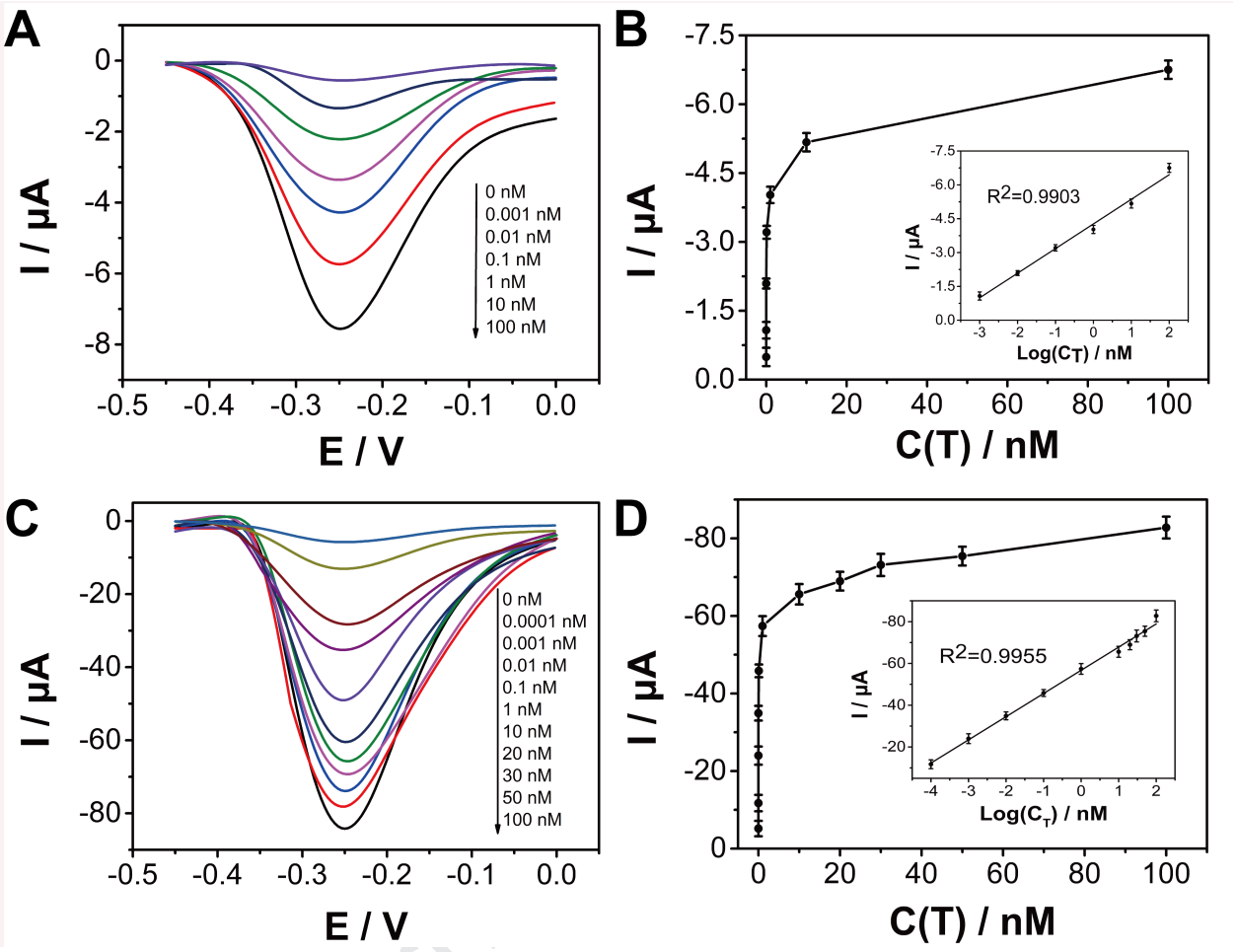
A
I / μA
E / V
0 nM
0.001 nM
0.01 nM
0.1 nM
1 nM
10 nM
100 nM
B
I / μA
C(T) / nM
R2=0.9903
Log(CT) / nM
C
I / μA
E / V
0 nM
0.0001 nM
0.001 nM
0.01 nM
0.1 nM
1 nM
10 nM
20 nM
30 nM
50 nM
100 nM
D
I / μA
C(T) / nM
R2=0.9955
Log(CT) / nM

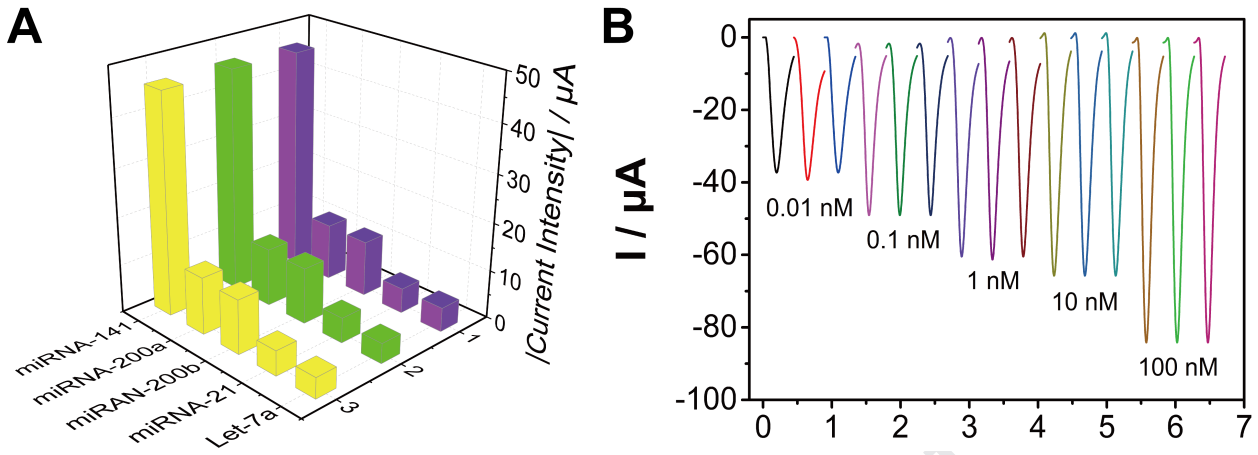

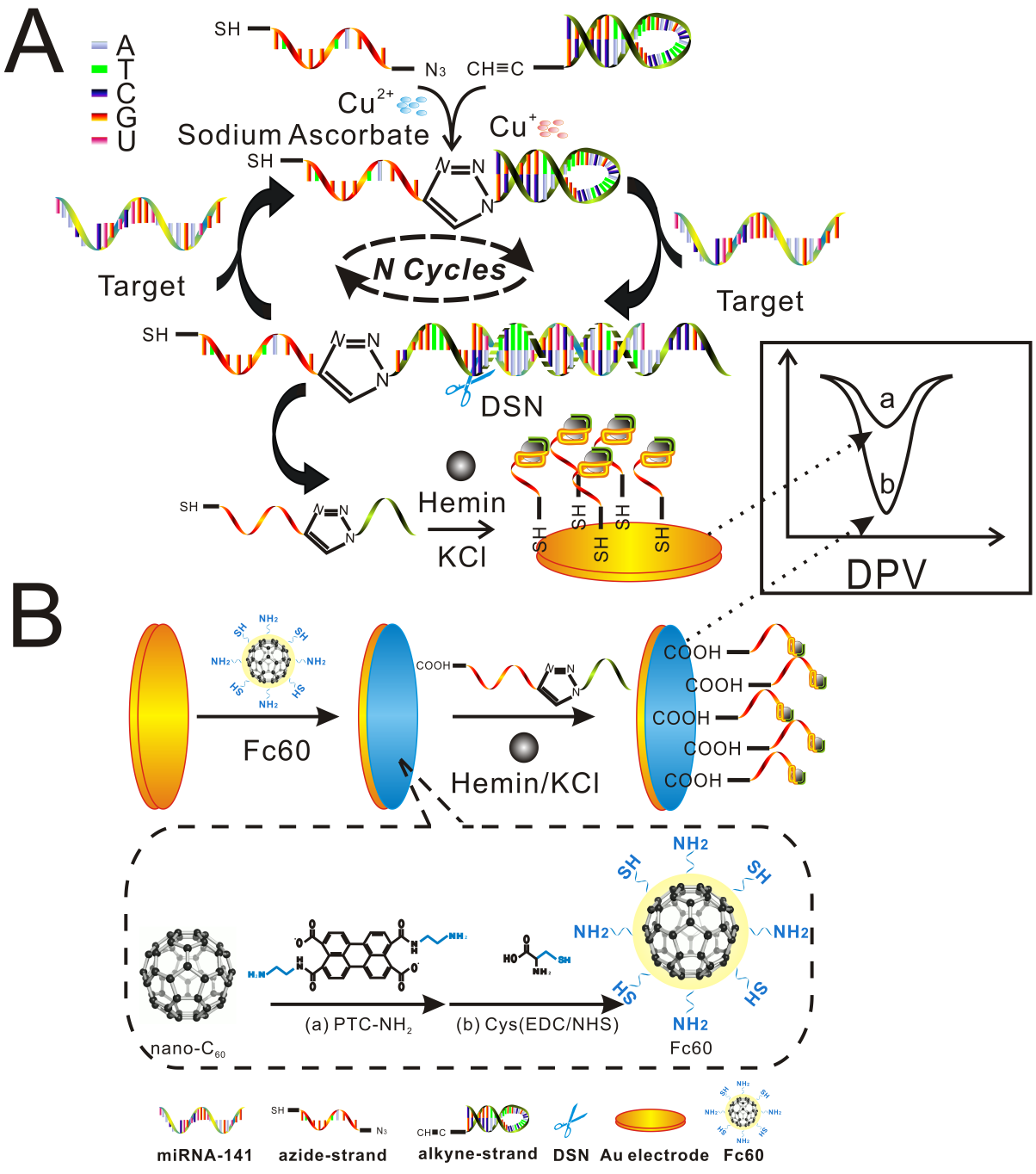
A
A
T
C
G
U
SH
N3
CH≡C
Cu2+
Sodium Ascorbate
Cu+
Target
N Cycles
Target
DSN
Hemin
KCl
a
b
DPV
B
Fc60
COOH
Hemin/KCl
nano-C60
(a) PTC-NH2
(b) Cys(EDC/NHS)
Fc60
miRNA-141
azide-strand
alkyne-strand
DSN
Au electrode
Fc60

- Click chemistry was used to high efficiency conjugation of nucleic acid strand.
- Rational application of DSN enzyme to achieve enzyme-assisted target recycling (EATR).
- Multi-functionalized fullerene nanoparticles were used to further amplify the detection signal.
- The established electrochemical biosensor displayed high sensitivity, specificity and universality.

Declaration of interests

☒ The authors declare that they have no known competing financial interests or personal relationships that could have appeared to influence the work reported in this paper.

☐The authors declare the following financial interests/personal relationships which may be considered as potential competing interests: